

# IDENTIFYING DAMAGE IN MULTIDIRECTIONAL GFRP COMPOSITE LAMINATES USING THERMOELASTIC STRESS ANALYSIS

I. Jiménez-Fortunato<sup>1</sup>, A. Quinlan<sup>2</sup> and \*J.M. Dulieu-Barton<sup>3</sup>

<sup>1</sup>School of Engineering, University of Southampton, Southampton, UK, <sup>2</sup>Western Michigan University, Department of Mechanical and Aerospace Engineering, USA <sup>3</sup>Bristol Composites Institute, University of Bristol, Bristol, UK,

\* Janice M. Dulieu-Barton (janice.barton@bristol.ac.uk)

**Keywords:** TSA, DIC, Damage identification

## ABSTRACT

A new three-axis subcomponent test set-up was developed to investigate the combined effect of web shear loading and local cross section deformation on the mechanical response and failure behaviour of a composite wind turbine blade spar cap to web T-joint. The representative subcomponent load case was extracted from a Finite Element model of the full blade subjected to pressure to suction side bending. Digital Image Correlation (DIC) and Thermoelastic Stress Analysis (TSA) were employed to capture the deformation of the T-joint specimen. A multicamera DIC system was selected to overcome limitations of a single stereo DIC system in imaging three-dimensional structures. To control and minimise heat convection in the measurement space between the cameras and the structure, fans were used to and shown to improve the DIC results. The novel loading and imaging procedures are developed and demonstrated on a “dummy” steel T-joint specimen with approximately equivalent stiffness to the composite T-joint. The steel T-joint was successfully subjected to realistic multiaxial loading and DIC and TSA results with good signal to noise ratios were obtained. A description of the test set up for the composite joint is provided based on the experience gained on the steel joint.

## 1 INTRODUCTION

Thermoelastic Stress Analysis (TSA) is a well-known full-field experimental stress analysis technique. The literature, e.g. [1-5] indicates that the stress induced thermoelastic temperature change ( $\Delta T$ ) for laminated polymer composites is dependent on the resin rich layer thickness, laminate type, the magnitude of the temperature change in the substrate layers and the loading frequency used for the tests, as these all influence heat transfer. In [5] the global and the ply-by-ply stresses were determined using DIC (Digital Image Correlation) measured strains from undamaged GFRP and CFRP laminates. The approach enabled  $\Delta T$  to be determined from the kinematics alone, i.e. without considering heat transfer. It was shown that for GFRP laminates  $\Delta T$  was not affected by ply-by-ply heat transfer; this was not the case for the CFRP laminates.

In the present work the GFRP (RP-528) laminates are studied. Two were cross-ply laminates, with stacking sequence  $[0,90]_{3S}$  and  $[90,0]_{3S}$ , with the same global stiffness but different surface ply orientation, and a shear dominated laminate,  $[\pm 45]_{3S}$ . Digital Image Correlation (DIC) is used provide an independent strain measurement to monitor stiffness changes as damage progresses in the multidirectional composites. The overall purpose is to investigate the possibility of using TSA to identify damage in realistic composite GFRP laminated composites used in wind turbine blade structures.

## 2 METHODOLOGY

For sinusoidal loading conditions, it is possible to apply the same algorithm to the strain data obtained from DIC as is used to extract the thermoelastic response from an IR image series for TSA. Hence, a least-squares fit to the sinusoidal data was used to obtain the thermoelastic response ( $\Delta T$ ) from TSA and

the change in strain ( $\Delta\varepsilon$ ) from DIC - “least-squares DIC” (LSDIC). The methodology follows the procedure shown in Fig. 1.

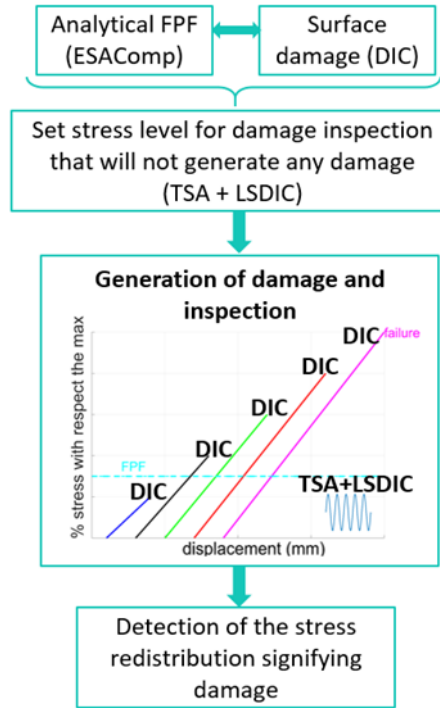


Figure 1 Methodology

The FPF was determined using ESAComp and used to determine the maximum cyclic load levels for the TSA. The specimens were damaged incrementally using quasi-static loading to different levels and images collected for DIC. Between each load increment the specimen was unloaded to the mean level of the cyclic load. Then during the cyclic loading, the TSA and LSDIC carried out. After which the specimen was removed from the test machine and inspected using X-ray CT-scans. This enabled damage evolution in the samples to be tracked at each load increment and help to understand what the failure mechanism is and how damage is initiated and evolved. After the X-ray images were collected, the specimen was returned to the test machine and loaded to the next load increment and then unloaded to the same mean load used in the previous TSA and LSDIC inspection and so on. A constitutive parameter,  $C$ , was extracted as follows:

$$C = \frac{\frac{\Delta T}{T_0}}{\Delta(\varepsilon_{xx} + \varepsilon_{yy})} \quad (1)$$

where  $\Delta T/T_0$  is an indication of the sum of principal stresses extracted from the TSA and  $\Delta(\varepsilon_{xx} + \varepsilon_{yy})$  is the sum of the principal strains extracted from the LSDIC.

The parameter  $C$  can be regarded as a stiffness metric. However, it is important to note that  $\Delta T/T_0$  is also coupled to the coefficients of thermal expansion ( $\alpha_1$  and  $\alpha_2$ ) and specific heat capacity at constant pressure ( $C_p$ ), both of which may change as damage progresses, and it has been shown earlier to be sensitive to fibre angle and fibre reorientation.

### 3 EXPERIMENTAL RESULTS

Figure 2 shows the  $\Delta T/T_0$  average across the specimen plotted against the homogenised stress applied to the laminate in each loading step, indicated as the ‘damaging stress’ on the x axis of the plot. The three different laminates and three different loading frequencies are shown. It is important to remember that the load range applied to each of these samples is the inspection load range. It can be seen that for the  $[0,90]_{3s}$  laminate,  $\Delta T/T_0$  is constant for each ‘damaging stress’ indicating that the specimen is not damaged. The  $[90,0]_{3s}$  laminate shows a slight reduction of  $\Delta T/T_0$  at higher stresses due to the surface resin-rich layer being degraded, as the  $90^\circ$  ply in contact with the resin-rich layer has been damaged at the last load steps. The degradation of the resin-rich layer is highlighted for the  $[\pm 45]_{3s}$  laminate as it suffers much more deformation when the stress increases, and hence, higher degradation in the resin-rich layer. The  $[\pm 45]_{3s}$  specimen did exhibit plastic deformation in the test coupon, where the coupon length elongated at higher stresses. Additionally, there is a linear reduction of  $\Delta T/T_0$  when the stress is higher than 83 MPa. Across all the three test specimens, the X-ray CT-scans did not show any damage except for the last scan of the  $[\pm 45]_{3s}$  laminate, where a crack was observed at the centre of the stacking sequence (Figure 3), but it was not visible in the TSA as there is no heat transfer occurring in the GFRP laminate. Full-field  $\Delta T$  for each specimen at the first and last damaging stresses are shown in Figure 4. It can be seen that the resin-rich layer has been damaged for the  $[90,0]_{3s}$  and the  $[\pm 45]_{3s}$  laminates as both specimens show an attenuation on  $\Delta T$  and cracks at the last damaging stress. However,  $[0,90]_{3s}$  laminate does not show any difference in the  $\Delta T$  field between the first and last damaging stress due to no heat transferring from the possible damaged subsurface  $90^\circ$  ply to the resin rich layer. Hence, it can be concluded that the  $[0,90]_{3s}$  laminate is not suitable to analyse damage progression as  $\Delta T/T_0$  was constant with respect to the damaging stress and no damage was seen in  $\Delta T$  field. Additionally,  $[90,0]_{3s}$  laminate only showed a change in  $\Delta T/T_0$  at the last damaging stress, which was confirmed by the  $\Delta T$  field, but did not show any damage progression as seen in the  $[\pm 45]_{3s}$  specimen.

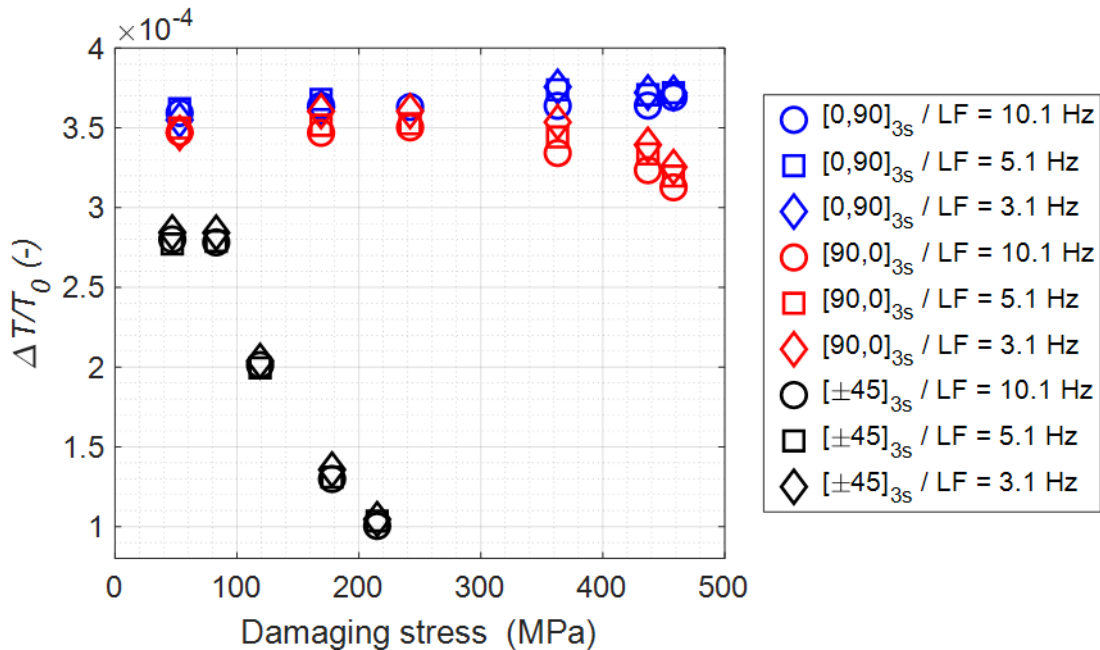
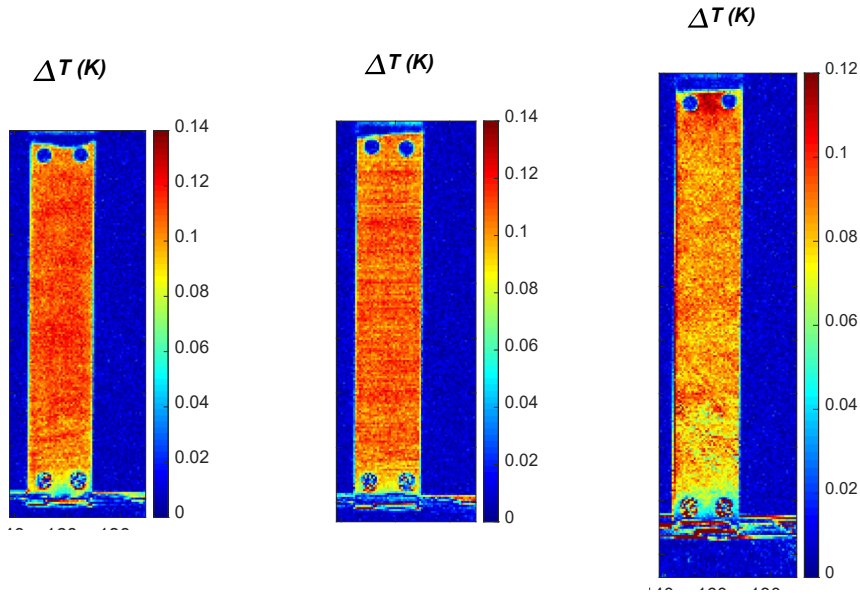


Figure 2 TSA results  $\Delta T/T_0$  vs damaging stress with loading frequency (LF)



Figure 3 Crack shown in centre of the stacking sequence  $[\pm 45]_{3s}$

(a)  $[0,90]_{3S}$  after 53 MPa (b)  $[90,0]_{3S}$  after 53 MPa (c)  $[\pm 45]_{3S}$  after 47 MPa



(d)  $[0,90]_{3S}$  after 458 MPa (e)  $[90,0]_{3S}$  after 458 MPa (f)  $[\pm 45]_{3S}$  after 215 MPa

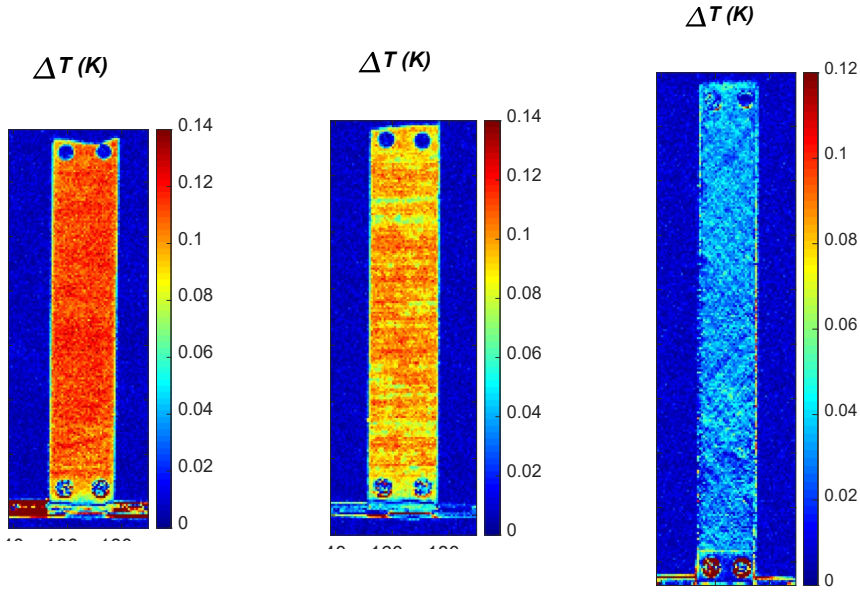


Figure 4 Full-field  $\Delta T$  at first (a)-(c) and last (d)-(f) damaging stresses at 5.1 Hz loading frequency

Figure 5 shows the LSDIC results for the three laminates and loading frequencies, in particular, the  $\Delta(\varepsilon_{xx} + \varepsilon_{yy})$  against the previous applied stress. It can be seen that for both cross-ply samples there are no changes in  $\Delta(\varepsilon_{xx} + \varepsilon_{yy})$  except at the last applied stress, where it is marginally reduced. Therefore, the stiffness of both cross-ply laminates remain almost unchanged throughout the damaging stress. However, regarding the  $[\pm 45]_{3S}$  sample, there is a reduction in  $\Delta(\varepsilon_{xx} + \varepsilon_{yy})$  when the stress is higher than 83 MPa, which implies that the stiffness has changed. The change in stiffness of the  $[\pm 45]_{3S}$  laminate is due to the fibres reorienting towards the  $0^\circ$  ply by  $\sim 8^\circ$ . It is suggested that the  $[\pm 45]_{3S}$  laminate also suffers degradation of the coefficients of thermal expansion as presented in the literature [2, 3] due to possible micro-cracks taking place at the resin-rich layer that were not detected

on the CT-scans. It is evident in the TSA results as there is a steeper reduction in response when the stress increases, which is associated to the fibre reorientation and the degradation of the coefficients of thermal expansion.

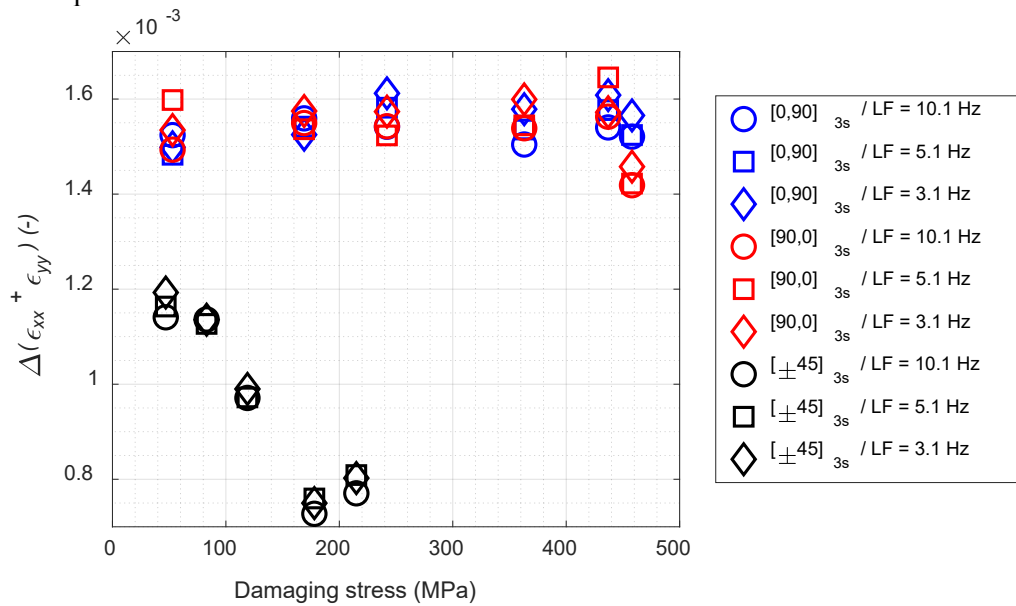


Figure 5 LSDIC results  $\Delta(\epsilon_{xx} + \epsilon_{yy})$  vs damaging stress

Figure 6 shows  $C$  plotted against the applied ‘stress’ (damaging force divided laminate cross section area) for a range of loading frequencies. It can be seen the loading frequency has little effect confirming the findings of [5]. For both cross-ply samples,  $[0,90]_{3s}$  and  $[90,0]_{3s}$ , the  $C$  remains almost constant with increasing levels of applied stress, while the  $[\pm 45]_{3s}$  sample presents a reduction of the constitutive parameter when the stress is over 83 MPa. The results are intriguing as the stiffness appears to reduce with damage in the  $[90,0]_{3s}$  and the  $[\pm 45]_{3s}$ . The X-ray CT showed that there was significant reorientation of the fibres in the  $[\pm 45]_{3s}$  laminate towards  $0^\circ$ . Hence,  $C$  is mainly driven by subsequent increased stiffness, and reduces the strains and decreased  $\Delta T/T_0$ . The reduction in  $\Delta T/T_0$  could be due to the matrix coefficient of thermal expansion being reduced due to possible micro-cracking, although these were not visible in the CT-scans. More importantly as the fibres re-orientate  $\alpha_1$  and  $\alpha_2$  will change. For the  $[90,0]_{3s}$  laminate there is a reduction in  $C$  at the larger loads and this could be attributed to gross cracking of surface ply. The  $[0,90]_{3s}$  the laminate shows no change in  $C$  indicating the cracking of the subsurface  $90^\circ$  plies has little effect on the laminate stiffness.

## CONCLUSIONS AND FUTURE WORK

The simultaneous use of DIC with TSA allows a constitutive parameter to be developed that may be used as a damage indicator in laminated composite materials. A generalised model is under development that can account for variations in material properties due to damage. This is currently being applied to both the well characterised RP-528 laminates and to a material representative of that used in wind blades.

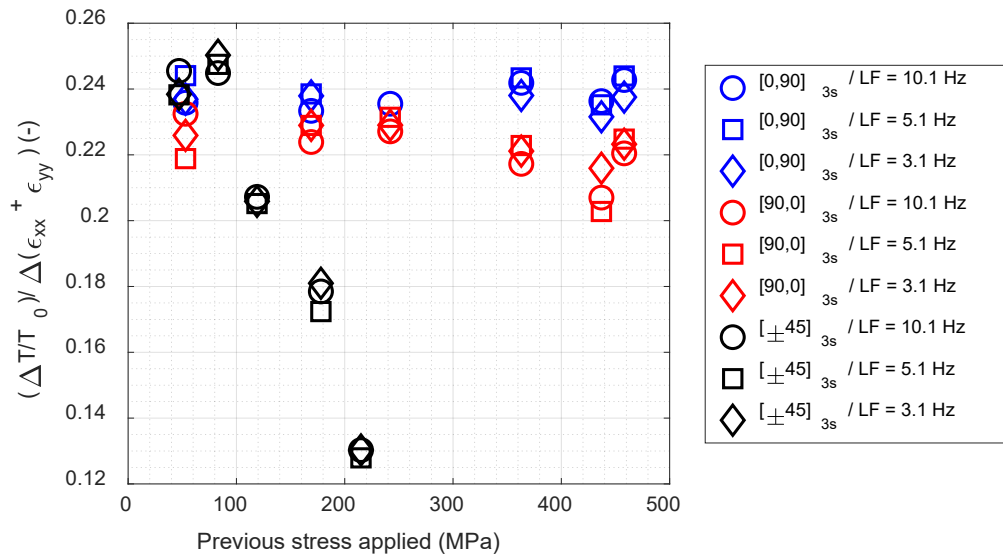


Figure 6 Constitutive parameter plotted against damage severity

### ACKNOWLEDGEMENTS

This work was supported by the Engineering and Physical Sciences Research Council [grant number EP/P006701/1], as part of the EPSRC Future Composites Manufacturing Research Hub. The experimental work described in the paper was conducted in the Testing and Structures Research Laboratory (TSRL) at the University of Southampton. The authors acknowledge the support received from Dr Andy Robinson, the TSRL Principal Experimental Officer.

### REFERENCES

- [1] P. R. Cunningham, J. M. Dulieu-Barton, A. G. Dutton, and R. A. Sheno, "The effect of ply lay-up upon the thermoelastic response of laminated composites", *Key Engineering Materials*, Conference Paper vol. 221-222, pp. 325-336, 2002.
- [2] G. Pitarresi, A. Conti, and U. Galietti, "Investigation on the Influence of the Surface Resin Rich Layer on the Thermoelastic Signal from Different Composite Laminate Lay-Ups", *Applied Mechanics and Materials*, vol. 3-4, pp. 167-172, 2006.
- [3] R. K. Fröhmann, S. Sambasivam, J. M. Dulieu-Barton, and S. Quinn, "Material Properties for Quantitative Thermoelastic Stress Analysis of Composite Structures", *Applied Mechanics and Materials*, vol. 13-14, pp. 99-104, 2008.
- [4] S. Sambasivam, S. Quinn, and J. M. Dulieu-Barton, "Identification of the source of the thermoelastic response from orthotropic laminated composites", in *ICCM17*, UK, 2009.
- [5] I. Jiménez-Fortunato, D. J. Bull, O. T. Thomsen, and J. M. Dulieu-Barton, "On the source of the thermoelastic response from orthotropic fibre reinforced composite laminates," *Composites Part A*:vol. 149, 2021, 106515.